Avarmaa, Katri; Strengell, Dan; Johto, Hannu; Latostenmaa, Petri; O'Brien, Hugh; Taskinen, Pekka

Solubility of Chromium in DON Smelting

Published in:
Mineral Processing and Extractive Metallurgy Review

DOI:
10.1080/08827508.2020.1854251

Published: 01/01/2022

Document Version
Publisher's PDF, also known as Version of record

Mineral Processing and Extractive Metallurgy Review
An International Journal

ISSN: (Print) (Online) Journal homepage: https://www.tandfonline.com/loi/gmpr20

Solubility of Chromium in DON Smelting

Katri Avarmaa, Dan Strengell, Hannu Johto, Petri Latostenmaa, Hugh O'Brien & Pekka Taskinen

To cite this article: Katri Avarmaa, Dan Strengell, Hannu Johto, Petri Latostenmaa, Hugh O'Brien & Pekka Taskinen (2022) Solubility of Chromium in DON Smelting, Mineral Processing and Extractive Metallurgy Review, 43:2, 201-208, DOI: 10.1080/08827508.2020.1854251

To link to this article: https://doi.org/10.1080/08827508.2020.1854251

Published online: 06 Dec 2020.

MINERAL PROCESSING AND EXTRACTIVE METALLURGY REVIEW
2022, VOL. 43, NO. 2, 201–208
https://doi.org/10.1080/08827508.2020.1854251

Taylor & Francis
Taylor & Francis Group

Solubility of Chromium in DON Smelting

Katri Avarmaa[a], Dan Strengell[a,b], Hannu Johto[c,d], Petri Latostenmaa[c], Hugh O'Brien[e], and Pekka Taskinen[a]

[a]Department of Chemical and Metallurgical Engineering, Aalto University, School of Chemical Technology, Espoo, Finland; [b]Gasum Oy, Espoo, Finland; [c]Boliden Harjavalta, Harjavalta, Finland; [d]Metso Outotec, Espoo, Finland; [e]Geological Survey of Finland, Espoo, Finland

ABSTRACT

Chromia-bearing raw materials in nickel and copper matte smelting are difficult to process due to their tendency of forming solid chromite spinel precipitates, leading to formation of mushy slag and buildups in the smelting vessel. The solubility of chromia in smelting slags, and especially in mattes, are not known accurately and new data for iron-silicate slags in equilibrium with low-iron nickel mattes have been measured at 1350–1450°C. Typical copper-bearing nickel mattes with Ni:Cu≈2 (w/w) in the DON (Direct Outotec Nickel) process with 2 to 10 wt% $[Fe]_{matte}$ have been equilibrated in carefully controlled S_2-O_2-SO_2-Ar gas atmosphere experiments with the corresponding silica saturated iron-silicate slags. The phase assays post quenching were measured by electron probe X-ray microanalysis, including the molten slag and matte as well as the solid phase of chromite spinel. Laser ablation ICP mass spectrometry was used to measure the trace elements in the matte. An additional variable in the slag composition was magnesia concentration, varying from zero to 10 wt% $(MgO)_{slag}$. The solubility of chromium in the slag at 1400°C was ≈0.7 wt% (Cr) and in the nickel matte 30–100 ppm [Cr], depending on the iron concentration of the sulfide matte. The impact of MgO on the chromium concentration in slag was small and within the experimental error of the measurements.

KEYWORDS

Nickel; sulfide matte; slag; thermodynamics

Introduction

Nickel matte smelting is chemically close to copper matte smelting and their fluxing practices are essentially the same (Font, Hino and Itagaki 2001; Kellogg 1987). Nickel sulfide ores are generally mineralogically and geochemically distinct from copper sulfide ores. Besides the often lower content of sulfides, the nickel concentrates contain silicate gangue materials rich in MgO and in certain cases also Cr_2O_3, i.e. traces of ferrochromite (Cramer 2001). These features make the primary smelting operation very demanding, due to the higher liquidus temperature of the slag and new dense compounds becoming stable in the operation and deporting as solid precipitates on the matte-slag interface in the smelting vessel (Barnes and Newall 2006; Nell 2004; Ritchie and Eksteen 2011).

Limited experimental studies have been conducted to investigate chromium behavior in iron-silicate slags and matte systems in nickel and copper matte smelting conditions. Kwatara (2006) studied chromium in copper matte – slag system under various pS_2 and pO_2 conditions at 1300–1500°C, whereas Du Preez (2009) equilibrated Cu-Ni-Fe-S matte and iron-silicate slag with different additives (Al_2O_3, MgO, CaO) with $pO_2 = 10^{-8}$ atm and $pS_2 = 10^{-3.5}$ atm at 1550 °C. Additionally, De Villiers and Kleyenstüber (1984) investigated chromium equilibrium in iron matte – alumina/magnesia-containing iron-silicate slags at 1450°C. Wright, Jahanshahi and Sun (2009) instead studied the chromium distribution behavior in the matte – Pt-alloy system under reducing conditions of fixed $pS_2 = 2.5x10^{-5}$ atm and varying $pO_2 = 10^{-15}$–10^{-12} atm at 1400°C. Sukhomlinov et al. (2020) measured chromium dissolution in alumina/lime-containing iron-silicate slags under black copper smelting conditions at 1300°C. Henao, Hino and Itagaki (2001) determined the chromium distribution between a nickel alloy and FeO_x-MgO-SiO_2 slags at 1500–1600 °C at MgO saturation and calculated the activity coefficient of chromia in the slag.

In PGM extraction, high MgO and Cr_2O_3 concentrations in iron-nickel-copper concentrates of the Bushveld Complex require higher smelting temperatures than nickel matte smelting, close to 1600°C (Andrews 2005; Coetzee 2006; Eksteen, van Beek and Bezuidenhout 2011; Nell 2004; Nelson et al. 2019). This is most likely the case also elsewhere where the ore body contains chromite minerals (Maier and Groves 2011). Despite the industrial importance, very little fundamental data are available in the literature on the chemistry and phase equilibria of chromia in iron-silicate slags, as well as the combined effect of chromia and magnesia in smelting slags. Murck and Campbell (1986) studied the dissolution of chromium in iron-silicate slags at 1300–1500°C under various oxygen partial pressures. Similarly, Roeder and Reynolds (1991) did experimental research for basaltic melts at chromite saturation and as a function of oxygen partial pressure between 1200 and 1400°C. Eguchi, Uchida and Chiba (1977) measured the solubility of chromium in a solid iron – iron-silicate slag system at 1230–1400°C, providing solubility of Cr_2O_3 as 1.5, 3 and 5 wt% at 1230, 1300 and 1400°C, respectively. In the study by Nell (2004), the chromia solubility in iron-silicate slag increased at low pO_2, being >5 wt% (Cr_2O_3) with $pO_2 < 10^{-11}$ atm at 1550 °C. In addition, Chen, Jak and Hayes (2005) investigated the liquidus line at 1400–1600°C with 2 wt%

CONTACT Katri Avarmaa katri.avarmaa@gmail.com Department of Chemical and Metallurgical Engineering, Aalto University, School of Chemical Technology, Aalto 00076, Finland.

Cr_2O_3 at silica saturation. Ilyushechkin, Hayes and Jak (2015) determined phase equilibria in silica-spinel and silica-spinel-pyroxene saturation under air and reducing conditions at 1350–1490°C. They presented chromia solubilities between 0.2 and 0.5 wt% in the oxide slag at the oxygen partial pressures ($7.8*10^{-7}$-$2.7*10^{-4}$) generated with the volumetric ratio CO_2:H_2 = 132:1. According to Sommerville et al. (2004), a spinel of $(Mg,Fe)(Al,Cr,Fe)_2(O)_4$ was precipitated and the solubility of chromium in the molten silicate was 0.3–1.3 wt% Cr at 1350–1630°C. They reported also chromium bearing olivine $(Fe,Mg,Cr)_2SiO_4$ and pyroxene $(Fe,Mg,Cr)SiO_3$ to be stable below 1450°C as primary phases. In reducing conditions and iron-free slags related to ferrochromium smelting, intensive experimental and modeling studies have been conducted in the literature, for example Curr, Wedepohl and Eriç (1988), Xiao and Holappa (1993), Pan and Eric (2004), Arnout et al. (2009) and Albertsson et al. (2013). Several papers are also available on the Cr^{2+}/Cr^{3+} and Cr^{3+}/Cr^{6+} equilibria in various slags (Farges 2009; Hanson and Jones 1998).

The aim of the present study was to determine the equilibrium solubility of chromium in DON (direct Outotec nickel) slags at typical iron concentrations (2–10 wt%) of the DON matte (Mäkinen and Ahokainen 2009) and to quantify the distribution of chromium between the matte and iron-silicate sags with varying MgO concentrations at silica and chromite spinel saturations. The measurements were carried out at a fixed SO_2 partial pressure of 0.1 atm that is generally used in the matte-slag studies and is based on the sulfur-oxygen potential diagram, i.e., Yazawa diagram (Yazawa 1974). The temperature range between 1350 and 1450°C was selected based on industrial practices of nickel matte smelting where the magnesia concentration of the feed mixture and thus that of the slag determines the practical slag tapping temperature (Mäkinen and Taskinen 2008).

Materials and methods

The experimental techniques included a high-temperature equilibration at controlled temperature and CO-CO_2-SO_2-Ar gas atmosphere, quick drop-quenching to an ice water mixture and direct phase analysis by electron probe X-ray microanalysis (EPMA) and laser ablation high resolution inductively coupled mass spectrometry (LA-HR-ICP-MS). Nickel matte was equilibrated with iron-silicate slag in silica crucibles in a temperature range of 1350–1450°C and matte grade range of 2–10 wt% [Fe]. This paper is a continuation of our previous work (Strengell et al. 2016) where we presented and discussed the results for nickel and matte phases in the DON process. The same experimental technique and assembly were used in this study as those described in detail in Strengell et al. (2016).

The experiments were carried out in a vertical tube furnace (Lenton PTF 15/45/450) employing controller unit of Eurotherm 3216 PID. The temperature was followed and measured during the experiments next to the sample with a calibrated S-type Pt/90%Pt–10%Rh thermocouple (Johnson-Matthey, UK; accuracy ± 2°C) and the ambient room temperature with a calibrated Pt100 sensor (Platinum Resistance Thermometer; SKS Group, Finland).

An equal amount (0.05 g/each) of premixed Cu_2S-FeS-Ni_3S_2 matte and Fe_2O_3-SiO_2-MgO-Cr_2O_3 slag were equilibrated in silica crucibles under controlled partial pressures of pS_2, pO_2 and pSO_2 at fixed temperature. All the aforementioned materials used were commercially available pure, high-grade reagents (>99.5%) supplied by Umicore, Alfa-Aesar or Sigma-Aldrich. The partial pressure of sulfur dioxide was held constant at 0.1 ± 0.01 atm and the partial pressures of O_2 and S_2 were fixed to a certain target 'matte grade' in each experiment, calculated using MTDATA software (databases of MTOX and SGTE pure substance) (Davies et al. 2002), see Table 1 for the used gas flows and corresponding pO_2 and pS_2. Inert argon was added to the gas mixture in order to increase the flow rate and N_2 post-experiment for flushing. The reactive gases of CO_2, CO and SO_2 were controlled by accurate mass-flow controllers (Aalborg DFC26, USA, accuracy of ±1% from full range) and were also calibrated employing a bubble-o-meter device (Dublin, OH). The inert gases of Ar and N_2 were controlled by rotameters (Aalborg 052–01-SA, USA; accuracy ± 2%). The use of silica crucible created silica saturation and the addition of Cr_2O_3 was 2 wt% (0.002 g/sample) to ensure spinel saturation. A 4-h equilibration time was shown to be sufficient to reach equilibrium (results presented in (Strengell et al. 2016)) and thus, employed in the experiments. After 4-h equilibrium the sample was quickly quenched and prepared by using metallographic techniques for preliminary SEM-EDS and primary EPMA and LA-HR-ICP-MS analyses.

Two identical experimental series were carried out to determine the concentration of chromium in slag and matte, as well as the matte-slag distribution coefficients. Each series contained nine experiments at 1400°C (three matte grades with three MgO concentrations), and three experiments at 1350 and 1450°C, respectively, at a constant 5 wt% [Fe] in matte with three MgO concentrations. In the following sections, parentheses () and [] refer to the slag and matte phases, respectively, except when examining the spinel result that are also presented with () parenthesis.

The primary phase analyses were executed using a Cameca SX100 EPMA (Cameca SAS, France) with wavelength dispersive spectrometers (WDS) housed at Geological Survey of Finland. The EPMA settings used, detection limits and standards have been presented earlier in detail (Strengell et al. 2016). The detection limit of chromium in the EPMA measurements were 125, 109, and 199 ppmw in matte, slag and spinel, respectively. The laser ablation single collector ICP-MS

Table 1. The used gas flows and their partial pressures at each experimental temperature.

Temp/ °C	Target Fe in matte/ wt-%	MgO in slag/wt-%	log P_{O2}/ atm	log P_{S2}/ atm	CO/ mL min^{-1}	CO_2/ mL min^{-1}	SO_2/ mL min^{-1}	Ar/ mL min^{-1}
1350	5.0	0, 5 and 10	−7.25	−3.17	8	55	40	300
1400	2.5	0, 5 and 10	−6.74	−3.41	8	55	40	300
1400	5.0	0, 5 and 10	−6.91	−3.15	9.9	55	40	300
1400	10.0	0, 5 and 10	−7.18	−2.67	16	55	40	300
1450	5.0	0, 5 and 10	−6.67	−3.03	13.3	55	40	300

analyses of the mattes were executed by using a Nu AttoM SC-ICP-MS (Nu Instruments Ltd., Wrexham, UK) and an Analyte G2 193 nm ArF laser-ablation system (Teledyne CETAC Technologies, Omaha, USA). The laser was run at a pulse frequency of 10 Hz and a pulse energy of 4 mJ at 40% attenuation to produce an energy flux of 3 J/cm^2 on the sample surface. Mass1 and ^{57}Fe was used as external and internal standards, respectively, for quantification, and BCR2G and BHVO-2 G for quality control. The measurements were performed for Mg, Si, S, Cr, Ni and Pb at low resolution (M/ΔM = 300) using the fast scanning mode. The instrumental uncertainty of the LA-HR-ICP-MS technique was evaluated as ± 5–10 wt%. Eight analyses points per phase were measured with both analytical techniques, and the averages and standards deviations of those were calculated and used as results.

Results

The obtained chromium concentration of the slag at 1400°C as a function of iron concentration of the nickel matte is shown in Figure 1. The data were calculated averages of EPMA results from the glassy and originally molten part of the silicate slag.

The scatter and uncertainty of the observations were relatively large and it is difficult to conclude whether the oxygen partial pressure or MgO concentration in slag have an impact on the chromium solubility in the composition range investigated. At least the influence of MgO over the studied concentration rage was small.

The temperature dependence of chromium solubility at silica-spinel saturation is shown in Figure 2. The measured solubility tended to increase slightly with temperature, in spite of the severe increase in silica concentration which lowered the solubilities of several other metals in iron-silicate slags, as indicated by Takeda (1997) and Park et al. (2011). This was particularly true in high-iron slags with less than 30 wt% (SiO_2), i.e. on the basic regions away from the orthosilicate composition of the Fe-O-SiO_2 system. Again, experimental scatter was relatively large.

The saturation phase of chromia in the slag was a spinel-type solid solution in all MgO concentrations of the slag. It had higher density than the molten bulk slag which characterized its deportment in smelting vessels (Barnes and Newall 2006). The composition of the spinel as a function of the prevailing oxygen partial pressure and MgO activity of the slag changed as magnesia dissolved into the spinel from the slag. EPMA analyses indicated that the spinel did not contain copper oxide or silica. In the case of the alumina-bearing slags, the equilibrium spinels would dissolve alumina (Ilyushechkin, Hayes and Jak 2015; Klemettinen, Avarmaa and Taskinen 2017) but due to the low alumina levels in the DON slag, the synthetic slags used in this study and the spinels were free of alumina.

Distribution of chromium between spinel and slag is shown in Figure 3 at different magnesia concentrations at 1400°C and at different temperatures with about 5 wt% MgO in the slag. It was defined in the conventional way as:

$$L^{sp/s}Me=(wt\%Me)_{spinel}/(wt\%Me)_{slag} \quad (1)$$

where Me denotes the dissolved metal in the spinel (sp) and molten silicate slag (s) phases, respectively. It is a thermodynamic variable which is independent of the scale of the system and thus particularly suitable for industrial use. This thermodynamic relation (1) also results in an estimate of the uncertainties of the obtained distribution coefficients as:

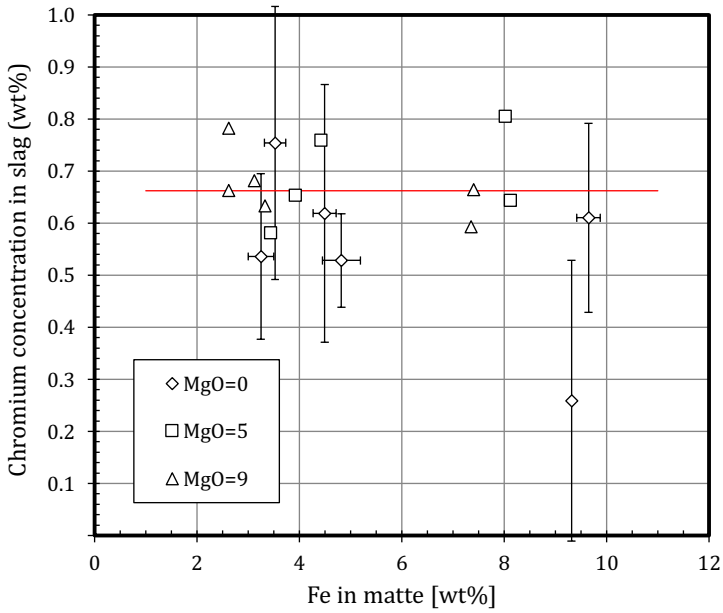

Figure 1. The obtained solubilities of chromium in molten iron-silicate slags at silica-spinel saturation as a function of iron concentration of nickel matte at 1400°C; the error bars show the standard deviations of the results with MgO = 0 in the slag and the red horizontal line shows the average value of all experimental points of 0.66 wt % (Cr).

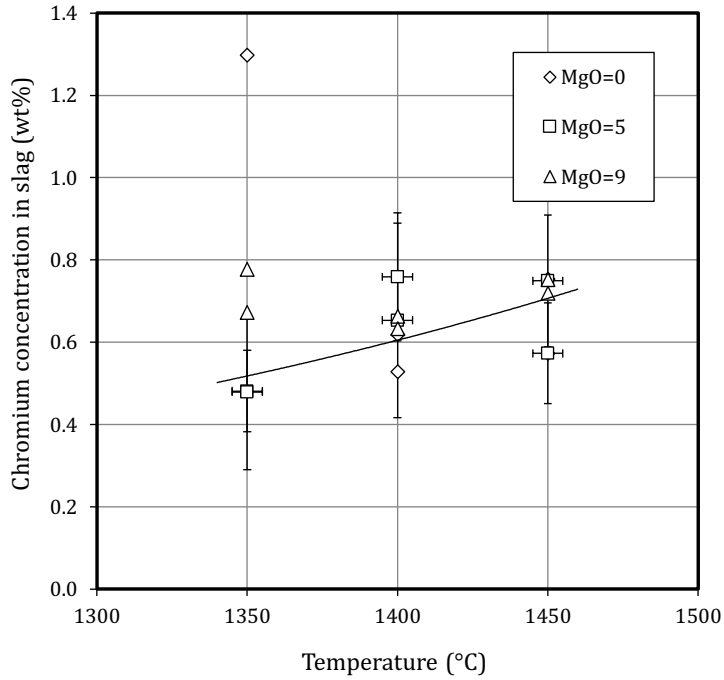

Figure 2. The impact of temperature on the chromium solubility in silica-spinel saturated, molten iron-silicate slags at 1350–1450°C and 5 wt% [Fe] in the DON matte; the trend line has been fitted to the points with 5 wt% (MgO).

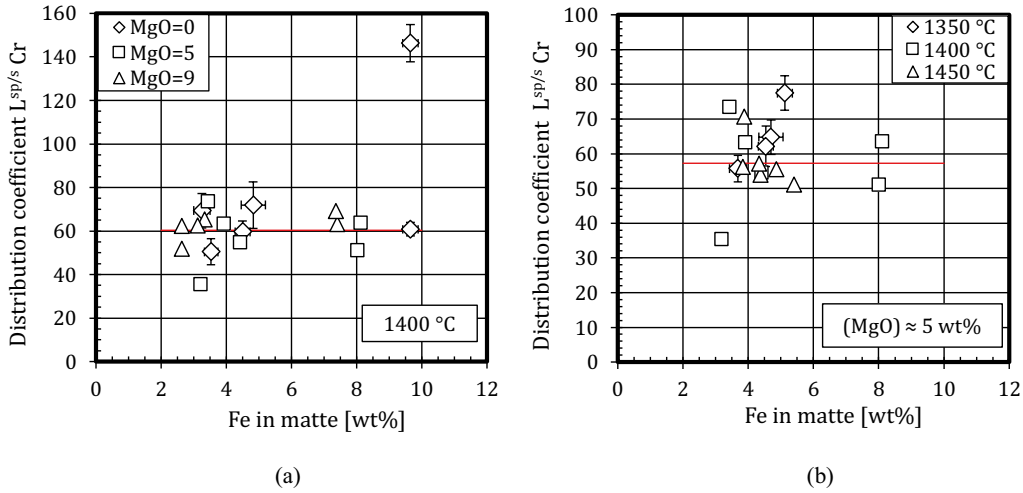

Figure 3. Distribution coefficient of chromium between spinel and molten slag (a) at 1400°C as a function of the iron concentration of the DON matte and (b) at 5 wt% MgO in the slag at 1350–1450°C; the error bars in (a) refer to the experimental data at 0 wt% MgO in the slag and in (b) at 1350°C. The red horizontal lines show the average of the experimental points presented in each diagram.

$$\Delta L = L \cdot \left\{ \Delta(Me)_{sp}/(Me)_{sp} + \Delta(Me)_{slag}/(Me)_{slag} \right\} \quad (2)$$

where $\Delta(Me)_{sp}$ is the standard deviation of EPMA measurement of the spinel and $\Delta(Me)_s$ is that in the slag, and L, $(Me)_{sp}$ and $(Me)_s$ are the distribution coefficient, solubility of Me in spinel and in slag, respectively.

The distribution coefficient obtained indicated that chromium was preferentially deporting in the solid spinel and thus it contained much more chromium than the average slag. No significant dependence could be seen between the distribution coefficient and iron concentration of the matte, nor the MgO concentration in slag and temperature.

The LA-HR-ICP-MS results of the matte domains allow an estimation of the chromium solubility in the nickel matte at silica-spinel saturation, Figure 4. The dissolved chromium concentrations in the matte were below the detection limit of EPMA but were at suitable levels for measurement by LA-HR-ICP-MS techniques as presented in Figure 4.

The only available data on chromium solubility in matte concerning slag-matte equilibrium in the literature are the ICP and EDS measurements by Kwatara (2006). Their values

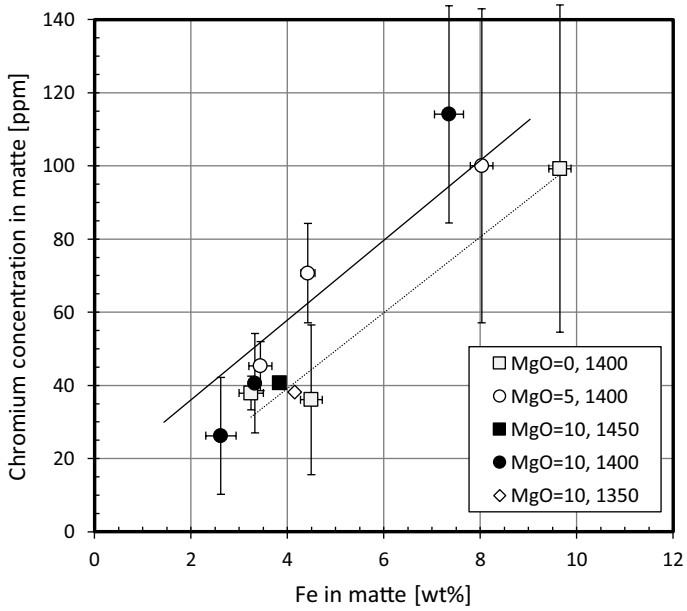

Figure 4. Measured solubilities of chromium in nickel mattes at 1350–1450°C analyzed by LA-HR-ICP-MS as a function of iron concentration of the DON matte analyzed by EPMA; symbols refer to various MgO concentrations of the slag (···· MgO = 0, – MgO = 5,10 wt%).

ranged from 0.3 wt% [Cr] to about 0.6 wt% [Cr] at 1300–1500°C by ICP analyses and with EDS they measured concentrations from 0 to 1 wt% [Cr] depending on the analyzed 'sub-phase' of the matte and the experimental conditions. The ICP-based concentrations were significantly higher than measured in the present study by the LA-HR-ICP-MS technique, whereas part of the EDS results by Kwatara (2006) were below the detection limits and could be in the same range as our results. The ICP technique requires manual phase separation and thus increased risk for distorted results as described by Fallah-Mehrjardi et al. (2017). The effect of MgO concentration in the slag seemed to have a small impact on the chromium solubility in the matte. Nevertheless, MgO had much greater influence on the activity of iron and thus on the composition of matte in the system.

The obtained matte-to-slag distribution coefficient of chromium is shown in Figure 5 at various MgO concentrations. The error bars were calculated in a similar way as presented in the distribution data for chromium between spinel and slag phase, according to Equation (2). As a function of iron concentration of matte, the distribution coefficient of chromium $L^{m/s}Cr$ increased slightly which indicated a small tendency for chromium to increase its solubility in the matte when oxygen pressure was lowered and sulfur pressure increased.

The current results indicated that from industrial point of view, the solubility of chromium in the sulfide matte of nickel smelting is negligible, and practically all chromium in the feed mixture of the primary smelting vessel in the DON process is deported in the slag, either as dissolved chromium oxide in the silicate slag or as high-density solid chromite. It is obvious that the composition of chromite spinel is a function of the spinel forming from the present slag components, such as alumina, nickel oxide, zinc oxide or magnesia (De Wilde et al. 2015).

The lattice structure of the spinel solution phase can be expressed as $(Me)(M)_2(O)_4$ where Me are predominantly divalent cations and M predominantly trivalent. If the deviations from cation:anion ratio of 3:4 are taken into account, the sublattice model of the spinel solution includes interstitial cations and vacancies in one or several cation sublattices (Barry et al. 1992). In this case, a simplified version was applied due to the relatively low experimental temperature where no major deviations from cation stoichiometry of 3:4 exist. The distribution of cations in spinel was calculated from mass balances, assuming that Mg and Ni are predominantly in the normal spinel location, i.e. in the first sublattice, and chromium in the second (Farges 2009). The results at 1400°C are shown in Figure 6 as a function of magnesia concentration in the slag. One can see that the dissolution of magnesia from the

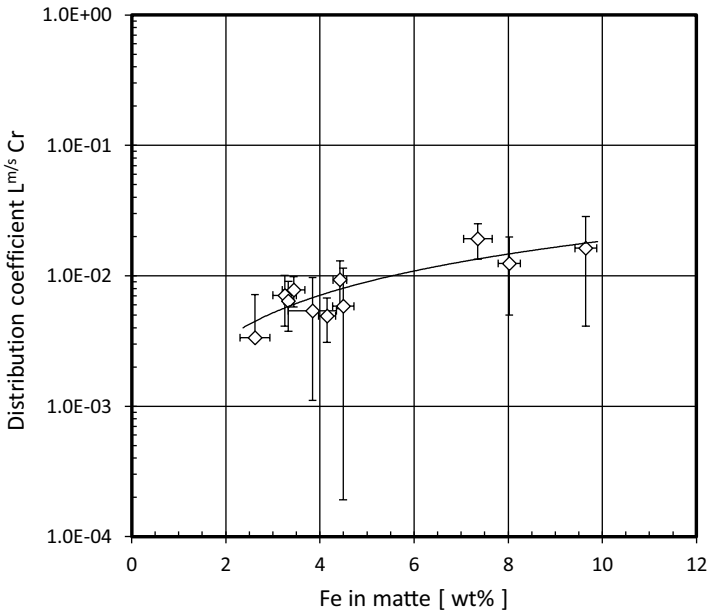

Figure 5. The distribution coefficient of chromium between nickel matte and iron-silicate slag at 1350–1450°C as a function of iron concentration of the DON matte; the various MgO concentrations of the slag cannot be distinguished from each other due to scattering in the distribution coefficient values.

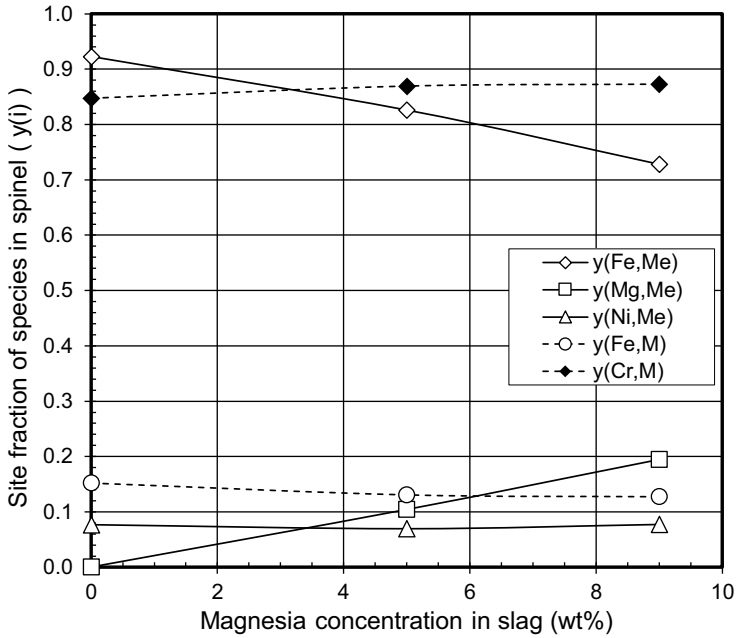

Figure 6. The estimated distributions of cations in the spinel $(Me)(M)_2(O)_4$ sublattices as a function of magnesia concentration of the bulk slag at silica-spinel saturation at 1400°C.

silicate into the spinel lattice gradually pushed iron from the inverse spinel location (Fe,M) in the octahedral sites to tetrahedral sites (Fe,Me).

Discussion and conclusions

The experimental results obtained in this study indicated that chromium (oxide) solubilities are small in iron-silicate slags at matte smelting temperatures and conditions used in nickel and copper smelting. An average concentration value of 0.66 wt% (Cr) or 0.96 wt% (Cr_2O_3) dissolving in the slag at double saturation of chromite spinel and silica at 1400°C was obtained in the current study. Although some experimental points included relatively big scatter, the overall trends and distribution coefficient results were very consistent providing reliability for the results.

The matte-slag equilibrium results obtained in this study were much lower than presented by Kwatara (2006) at 1300–1500°C. The distribution coefficients $L^{m/s}$ based on ICP measurements in Kwatara's study were between 0.07 and 0.13 depending on temperature, pO_2 and pS_2.

Bartie (2004) measured chromium distributions in the slag phase between different equilibrium phases at 1400–1600°C as a function of oxygen pressure. His slags contained about 5 wt% alumina and lime, and their magnesia concentrations varied from 15 to 20 wt% MgO. His results for chromium solubilities in slags and the distribution coefficients between spinel and slag are in good agreement with the present data at 1400°C. Roeder and Reynolds (1991) measured the solubility of chromium in a molten silicate at chromite saturation and as a function of oxygen partial pressure at 1200–1400°C. Their silicate was a low-iron, sulfur-free basalt, high in alumina and silica. The obtained chromium solubilities clearly increased with decreasing oxygen pressures and were clearly lower, about 0.1-0.2 wt% (Cr_2O_3) at $pO_2 = 10^{-7}$-10^{-8} atm and 1400°C. Sukhomlinov et al. (2020) reported chromium solubilities of 0.1–0.25 wt% at 1300°C and oxygen partial pressures of $pO_2 = 10^{-5}$–10^{-9} atm in ternary Fe-O-SiO_2 slags at silica-spinel saturation that are slightly on the lower side compared with the results achieved in this study.

The small distribution coefficient of chromium between the nickel matte and molten silicate slag at 1350–1450°C suggests that the expected carryovers of chromium from an electric furnace (EF) to the converting stage (e.g. Eksteen, van Beek and Bezuidenhout 2011) are due to slag and not matte transferred from EF to converters. The entrainment of slag into matte during tapping should then be avoided more carefully than today's practices permit. The current results also make possible to estimate the maximum chromium permitted in the feed mixture in order to avoid the formation of the buildups on the furnace walls and heart (Lennartsson et al. 2015). Due to the operational windows of copper matte smelting being close to that of DON smelting (Mäkinen and Taskinen 1998; Matousek 2014), the results obtained in the present study can be applied also in copper smelting operations.

Acknowledgments

The authors are thankful for Boliden Harjavalta for financially supporting this study. We would like to acknowledge the Geological Survey of Finland, its analytical facilities and staff, particularly and Mr. Lassi Pakkanen for conducting the EPMA measurements.

Disclosure statement

The authors declare that they have no known competing financial interests or personal relationships that could have appeared to influence the work reported in this paper.

ORCID

Katri Avarmaa http://orcid.org/0000-0002-8632-3788
Hugh O'Brien http://orcid.org/0000-0002-7900-579X
Pekka Taskinen http://orcid.org/0000-0002-4054-952X

References

Albertsson, G., L. Teng, B. Björkman, S. Seetharaman, and F. Engström. 2013. Effect of low oxygen partial pressure on the chromium partition in CaO-MgO-SiO_2-Cr_2O_3-Al_2O_3 synthetic slag at elevated temperatures. *Steel research International* 84 (7):670–79. doi:10.1002/srin.201200214.

Andrews, L. 2005. Factors affecting nickel recovery from slags produced during platinum smelting. *Mineral Processing and Extractive Metallurgy* 114 (3):C130–34. doi:10.1179/037195505X49750.

Arnout, S., M. Guo, I. Jung, B. Blanpain, and P. Wollants. 2009. Experimental determination of CaO-CrO-Cr_2O_3-MgO-SiO_2 and thermodynamic modeling of the CrO-Cr_2O_3-MgO-SiO_2 system. *Journal of the American Ceramic Society* 92 (8):1831–39. doi:10.1111/j.1551-2916.2009.03115.x.

Barnes, A. R., and A. F. Newall. 2006. Spinel removal from PGM smelting furnaces. In: P***roceedings*** *Southern African Pyrometallurgy 2006*, ed. R. T. Jones, 77–88. Johannesburg (RSA): SA IMM.

Barry, T. I., A. T. Dinsdale, J. A. Gisby, B. Hallstedt, M. Hillert, B. Jansson, S. Jonsson, B. Sundman, and J. R. Taylor. 1992. The compound energy model for ionic solutions with applications to solid oxides. *Journal of Phase Equilibria* 13 (5):459–75. doi:10.1007/BF02665760.

Bartie, N. J. 2004. The effects of temperature, slag chemistry and oxygen partial pressure on the behaviour of chromium oxide in melter slags. MSc thesis, Stellenbosch University, Dept Process Engineering, 137.

Chen, S., E. Jak, and P. Hayes. 2005. Effect of Al_2O_3 and Cr_2O_3 on liquidus temperatures in the cristobalite and tridymite primary phase fields of the MgO-'FeO'-SiO_2 system in equilibrium with metallic iron. *ISIJ International* 45 (6):798–06. doi:10.2355/isijinternational.45.798.

Coetzee, V. 2006. Common-sense improvements to electric smelting at impala platinum. *Journal of the Southern African Institute of Mining and Metallurgy* 106 (3):155–64.

Cramer, L. A. 2001. The extractive metallurgy of South Africa's platinum ores. *JOM* 53 (10):14–18. doi:10.1007/s11837-001-0048-1.

Curr, T. R., A. Wedepohl, and R. H. Eriç. 1988. The dissolution of a transvaal chromite in liquid silicate slags under neutral conditions between 1545 and 1660°C. In: *Proceedings of the 3rd* ***International*** *Conference on Slags and Fluxes*, University Strathclyde, Glasgow, 298–304. London (UK): The Institute of Metals, (printed 1989).

Davies, R. H., A. T. Dinsdale, J. A. Gisby, J. A. J. Robinson, and S. M. Martin. 2002. MTDATA-thermodynamic and phase equilibrium software from the national physical laboratory. *Calphad* 26 (2):229–71. doi:10.1016/S0364-5916(02)00036-6.

de Villiers, J. P. R., and A. S. E. Kleyenstüber. 1984. The partitioning of chromium between sulphide and silicate melts at controlled partial pressures of oxygen and sulphur. Report No. M139D, 16. Johannesburg (RSA): Mintek.

De Wilde, E., I. Bellemans, M. Campforts, A. Khaliq, K. Vanmeensel, D. Seveno, M. Guo, A. Rhamdhani, G. Brooks, B. Blanpain, et al. 2015. Wetting behaviour of Cu based alloys on spinel substrates in pyrometallurgical context. *Materials Science and Technology* 31 (15):1925–33. doi:10.1179/1743284715Y.0000000052.

Du Preez, R. C. 2009. Effect of lime additions and bulk chromium content on chromium deportment in smelter matte-slag systems. MSc thesis, Stellenbosch University, Dept Process Engineering, 101.

Eguchi, M., R. Uchida, and M. Chiba. 1977. Study of the fixing of chromium with iron-silicate slag (I). Phase equilibria of the FeO-Cr_2O_3-SiO_2 system in contact with metallic iron. *Tohoku Daigaku Senko Seiren Iho* 33 (1):24–30.

Eksteen, J. J., B. van Beek, and G. A. Bezuidenhout. 2011. Cracking a hard nut: An overview of Lonmin's operations directed at smelting of UG2-rich concentrate blends. In *Southern African pyrometallurgy 2011*, ed. R. T. Jones and P. den Hoed, 231–51. Johannesburg (RSA): SA IMM.

Fallah-Mehrjardi, A., T. Hidayat, P. C. Hayes, and E. Jak. 2017. Experimental investigation of gas/slag/matte/tridymite equilibria in the Cu-Fe-O-S-Si system in controlled atmospheres: Development of technique. *Metallurgical and Materials Transactions B* 48 (6):3002–16. doi:10.1007/s11663-017-1073-y.

Farges, F. 2009. Chromium speciation in oxide-type compounds: Application to minerals, gems, aqueous solutions and silicate glasses. *Physics and Chemistry of Minerals* 36 (8):463–81. doi:10.1007/s00269-009-0293-3.

Font, J., M. Hino, and K. Itagaki. 2001. Phase equilibrium between FeO_x-SiO_2 Base Slag and Cu_2S-Ni_3S_2-FeS matte with different Cu and Ni Contents at 1573 K. *Metallurgical Review of MMIJ* 17 (2):106–15.

Hanson, B., and J. H. Jones. 1998. The systematics of Cr^{3+} and Cr^{2+} partitioning between olivine and liquid in presence of spinel. *American Mineralogist* 83 (7–8):669–84. (July-August). doi:10.2138/am-1998-7-801.

Henao, H. M., M. Hino, and K. Itagaki. 2001. Distribution of Ni, Cr, Mn, Co and Cu between Fe-Ni Alloy and FeO_X-MgO-SiO_2 Base Slags. *MATERIALS Transactions* 42 (9):1959–66. doi:10.2320/matertrans.42.1959.

Ilyushechkin, A., P. C. Hayes, and E. Jak. 2015. Affects of Al_2O_3, CaO and Cr_2O_3 on liquidus temperatures of Fe-Mg-Si-O slags. *Canadian Metallurgical Quarterly* 54 (2):185–97. doi:10.1179/1879139514Y.0000000177.

Kellogg, H. H. 1987. Thermochemistry of Nickel-Matte converting. *Canadian Metallurgical Quarterly* 26 (4):285–98. doi:10.1179/cmq.1987.26.4.285.

Klemettinen, L., K. Avarmaa, and P. Taskinen. 2017. Slag chemistry of high-alumina iron silicate slags at 1300°C in WEEE smelting. *Journal of Sustainable Metallurgy* 3 (4):772–81. doi:10.1007/s40831-017-0141-5.

Kwatara, M. 2006. Chromium deportment in copper matte equilibrated with Cr_xO-containing slag. MSc thesis, Stellenbosch University, Dept Process Engineering, 117.

Lennartsson, A., F. Engström, B. Björkman, and C. Samuelsson. 2015. Characterisation of buildup in an electric furnace for smelting copper concentrate. *Canadian Metallurgical Quarterly* 54 (4):477–84. doi:10.1179/1879139515Y.0000000026.

Maier, W. D., and D. I. Groves. 2011. Temporal and spatial controls on the formation of magmatic PGE and Ni-Cu deposits. *Mineralium Deposita* 46 (8):841–57. doi:10.1007/s00126-011-0339-6.

Mäkinen, T., and T. Ahokainen. 2009. 50 years of nickel flash smelting – still going strong. In *Pyrometallurgy of Nickel and Cobalt 2009*, ed. J. Liu, et al, 209–20. Montreal: Canadian Inst. Min. Metall.

Mäkinen, T., and P. Taskinen. 1998. Physical chemistry of direct Nickel matte smelting. In *Sulfide smelting '98*, ed. J. A. Asteljoki and R. L. Stephens, 59–68. Warrendale (PA): TMS.

Mäkinen, T., and P. Taskinen. 2008. State of the art in nickel smelting: Direct Outokumpu nickel technology. *Mineral Processing and Extractive Metallurgy* 117 (2):86–94. doi:10.1179/174328508X290867.

Matousek, J. W. 2014. Oxidation Potentials in Matte Smelting of Copper and Nickel. *JOM* 66 (9):1670–76. doi:10.1007/s11837-014-1072-2.

Murck, B. W., and I. H. Campbell. 1986. The effects of temperature, oxygen fugacity and melt composition on the behaviour of chromium in basic and ultrabasic melts. *Geochimica et cosmochimica acta* 50 (9):1871–87.

Nell, J. 2004. Melting of platinum group metal concentrates in South Africa. *Journal of the Southern African Institute of Mining and Metallurgy* 100 (8):423–28.

Nelson, L. R., G. A. Georgalli, K. L. Hines, and R. J. Hundermark. 2019. Converter processing of platinum group metals. *Mineral Processing and Extractive Metallurgy Review* 128 (1–2):134–59.

Pan, X., and R. H. Eric. 2004. Chromium distribution between slag and non-carbon saturated metal phases under changing partial pressure of carbon monoxide. *Journal of the Southern African Institute of Mining and Metallurgy* 104 (11):583–87.

Park, J. G., H. S. Eom, W. W. Huh, Y. S. Lee, D. J. Min, and I. Sohn. 2011. A study in the thermodynamic behavior of Nickel in the MgO-SiO_2-FeO Slag system. *Steel research International* 82 (1):415–21. doi:10.1002/srin.201000151.

Ritchie, S., and J. J. Eksteen. 2011. Investigating the effect of slag bath conditions on the existence of multiphase emulsion zones in PGM

smelting furnaces using computational fluid dynamics. *Minerals Engineering* 24 (7):661–75. doi:10.1016/j.mineng.2010.09.017.

Roeder, P. L., and I. Reynolds. 1991. Crystallization of chromite and chromium stability in basaltic melts. *Canadian Metallurgical Quarterly* 32 (5):909–34. doi:10.1093/petrology/32.5.909.

Sommerville, M., S. Wright, S. Sun, and S. Jahanshahi. 2004. Liquidus temperature and viscosity of melter slags. In: *Proceedings VII International Congress on Molten Slags, Fluxes and Salts*, 219–24. Johannesburg (RSA): SA IMM.

Strengell, D., K. Avarmaa, H. Johto, and P. Taskinen. 2016. Distribution equilibria and slag chemistry of DON smelting. *Canadian Metallurgical Quarterly* 55 (2):234–42.

Sukhomlinov, D., K. Avarmaa, O. Virtanen, P. Taskinen, and A. Jokilaakso. 2020. Slag–copper equilibria of selected trace elements in black copper smelting. part I. Properties of the slag and chromium solubility. *Mineral Processing and Extractive Metallurgy Review* 41 (1):32–40. doi:10.1080/08827508.2019.1575212.

Takeda, Y. 1997. Copper solubility in matte smelting slags. In: Proceedings *Molten Slags, Fluxes and Salts '97 Conference*, 329–39. Warrendale (PA): The Iron & Steel Society.

Wright, S., S. Jahanshahi, and S. Sun. 2009. Behaviour of Cr in Cu-Fe-Ni -S mattes. In: *Molten 2009 Conference* ed. M. Sanches, R. Parra, G. Riveros, and C. Diaz, 632–41. Santiago (Chile): Ch IMM, CD-ROM.

Xiao, Y., and L. Holappa. 1993. Determination of activities in slags containing chromium oxides. *ISIJ International* 33 (1):66–74. doi:10.2355/isijinternational.33.66.

Yazawa, A. 1974. Thermodynamic considerations of copper smelting. *Canadian Metallurgical Quarterly* 13 (3):443–53. doi:10.1179/cmq.1974.13.3.443.